

## GIANT OPTICAL ACTIVITY AND NEGATIVE REFRACTIVE INDEX USING COMPLEMENTARY U-SHAPED STRUCTURE ASSEMBLY

Y. Z. Cheng, Y. Nie, and R. Z. Gong\*

School of Optical and Electronic Information, Huazhong University of Science and Technology, Wuhan 430074, China

**Abstract**—In this paper, a chiral metamaterial (CMM) with complementary U-shaped structure assembly is proposed. The microwave experimental and simulated results of the proposed complementary structure exhibit giant optical activity. The experimental results are in good agreement with the numerical ones. The retrieval results reveal that negative refractive indices for right-handed and left-handed circularly polarized waves could be easily realized due to strong chirality. The mechanism of the chiral behaviors of resonance frequencies will be illustrated by simulated current distributions. Further, the complementary U-shaped structure assembly also exhibits stronger circular dichroism, giant optical activity, and negative index at near-infrared region by simulations.

### 1. INTRODUCTION

Metamaterial (MM) is a novelty material and designated by manipulating extreme magnitudes of physical conditions during synthesis and manufacture, which attains its properties from unit structure rather than constituent materials [1]. Since the negative index properties of MMs was experimentally demonstrated by Smith et al. [2, 3], MMs have become an excellent platform for some unique applications, such as superlens, cloaking, electric devices, and so on [4–7]. Thus, MMs have attracted considerable interest in many research fields of science and technology, which has been growing rapidly in recent years. Usually, negative indices of MMs are obtained by adjusting the permittivity and permeability to be negative simultaneously. Some artificial structures, such as SRRs and wire [3],

---

*Received 4 July 2012, Accepted 16 August 2012, Scheduled 22 August 2012*

\* Corresponding author: Rong Zhou Gong (rzhgong@mail.hust.edu.cn).

fishnet [8], rod pairs [9], crosses [10] were proposed and easier to achieve simultaneously negative permittivity and permeability. Recently, an alternative route to achieve negative refraction by utilizing material chirality has been theoretically proposed and investigated [11, 12]. Chiral MMs are artificial materials that lack any planes of mirror symmetry, so that there is cross-coupling between the electric and magnetic fields at the resonance. Owing to its interesting properties (such as the giant optical activity and circular dichroism), which possess great interest to many areas of science, for example, analytical chemistry and molecular biology. Thus, the chiral MMs have attracted much attention [13–19]. Various enantiomeric forms or similar bi-layer chiral structure, such as Twisted-Rosettes [20, 21], Twisted-Crosswires [22, 23], Four-U-SRRs [24, 25], and Conjugate-Swastikas [26], complementary structure [27] and other novel structures [28–31] have been proposed and investigated, which can obtain optical activity, circular dichroism, and negative refractive index [32].

For homogenous CMMs, the degeneracy of the two circularly polarized waves is broken, i.e., refractive indices of right-handed circularly polarized (RCP, +) waves and left-handed circularly polarized (LCP, -) waves are different. For convenience and assuming  $e^{-i\omega t}$  as time dependence, the constitutive relations can be written as [33],  $\mathbf{D} = \varepsilon_0 \varepsilon \mathbf{E} + (i\kappa/c_0) \mathbf{H}$ ,  $\mathbf{B} = (-i\kappa/c_0) \mathbf{E} + \mu_0 \mu \mathbf{H}$ , where  $\varepsilon_0$  and  $\mu_0$  are the permittivity and permeability of vacuum,  $\varepsilon$  and  $\mu$  are the relative permittivity and permeability of the CMMs,  $c_0$  is the speed of light in vacuum,  $\kappa$  is chiral parameter. The RCP (+) wave and LCP (-) wave are defined as  $\mathbf{E}_{\pm} = (1/\sqrt{2}) \mathbf{E}_0 (\hat{x} \pm i\hat{y})$ . The refractive indices for RCP and LCP waves can be expressed as  $n_{\pm} = n \pm \kappa$ , which implies that strong enough chirality parameter  $\kappa$  is required to achieve negative refraction for one circular polarization in principle [21], where  $n_+$ ,  $n_-$ ,  $n$  is the refractive index for RCP and LCP waves and average refractive index. At the same time, both RCP and LCP waves have the same impedance of  $z = \sqrt{\mu/\varepsilon}$ . For the chiral media constitutive relations, three important parameters will be defined respectively [33]. The first one is the optical (EM) activity, which could rotate the polarization plane of a linearly polarized wave propagating through it, and described as polarization azimuth rotation angle  $\theta = [\arg(T_{++}) - \arg(T_{--})]/2$  [33]. The second is the circular dichroism ( $\Delta = |T_{++}| - |T_{--}|$ ), which defines the different absorptivity of a RCP and LCP polarized wave inside the CMMs. The last is the ellipticity expressed as  $\eta = \arctan [(|T_{++}| - |T_{--}|)/(|T_{++}| + |T_{--}|)]$ , which defines the difference of polarization state of transmitted waves and incident waves [33], where  $T_{++}$ ,  $T_{--}$ ,  $\arg(T_{++})$  and  $\arg(T_{--})$  are

the magnitude and phase of the transmission coefficients for the RCP and LCP waves, respectively.

In this work, we designed a novel CMM using complementary U-shaped structure assembly of mutually twisted planar metal patterns in parallel planes, which supports a wealth of useful EM properties including giant optical activity and negative refraction. The experimental results are in good agreement with the numerical results. The further simulated results indicate that the complementary U-shaped structure assembly by selecting geometric parameters properly also exhibits stronger circular dichroism, giant optical activity, and negative index at near-infrared region.

## 2. PHYSICAL MODEL, SIMULATION AND EXPERIMENT FOR MICROWAVE FREQUENCY BAND

Babinet's principle would be applied to the MMs design, resulting in both a complementary spectral response and field [26, 34–36]. From microwave to visible frequencies, the U-shaped structure has been investigated widely. Negative index, optical activity, circular dichroism and other exotic EM properties could be achieved by proper structural assembly [16, 24, 25, 32, 37]. Generally, the unit cell of U-shaped CMMs is formed by four of these pairs, wherein the pairs are rotated by  $0^\circ$ ,  $90^\circ$ ,  $180^\circ$ , and  $270^\circ$  with respect to the EM wave propagation direction [25]. Here, our designed chiral MM is composed of a two-dimensional periodic array of complementary U-shaped copper foils assembly separated by a dielectric slab, and one of the unit cells is shown in Figure 1(a). The overall unit structure has fourfold rotational symmetry, not any mirror plane and center of inversion.

The numerical simulations were performed based on finite element method by using the frequency domain solver of the CST Microwave Studio. In all simulations, the unit cell boundary condition was applied and the circular polarized eigenwaves (LCP and RCP waves) were used directly. For experiments, the designed structure was fabricated with the optimized structure parameters by the conventional PCB technology. The layout of the designed complementary chiral MM (CCMM) is shown in Figure 1(b), a  $25 \times 25$  array of the complementary U-shaped resonator pairs is patterned on each side of the FR-4 dielectric board, and the final dimension of the fabricated sample is  $200 \text{ mm} \times 200 \text{ mm} \times 1.072 \text{ mm}$ . The geometry parameters of the unit cell are given as  $p = 8 \text{ mm}$ ,  $l = 2.8 \text{ mm}$ ,  $g = 0.6 \text{ mm}$ ,  $w = 1.2 \text{ mm}$ , and  $t_s = 1 \text{ mm}$ , and the thickness of copper is  $0.036 \text{ mm}$ . The relative dielectric constant of the FR-4 dielectric board is  $\varepsilon = 4.1$  with a dielectric loss tangent of  $0.02$ , and the conductivity of the copper is  $\sigma = 5.8 \times 10^7 \text{ S/m}$ .

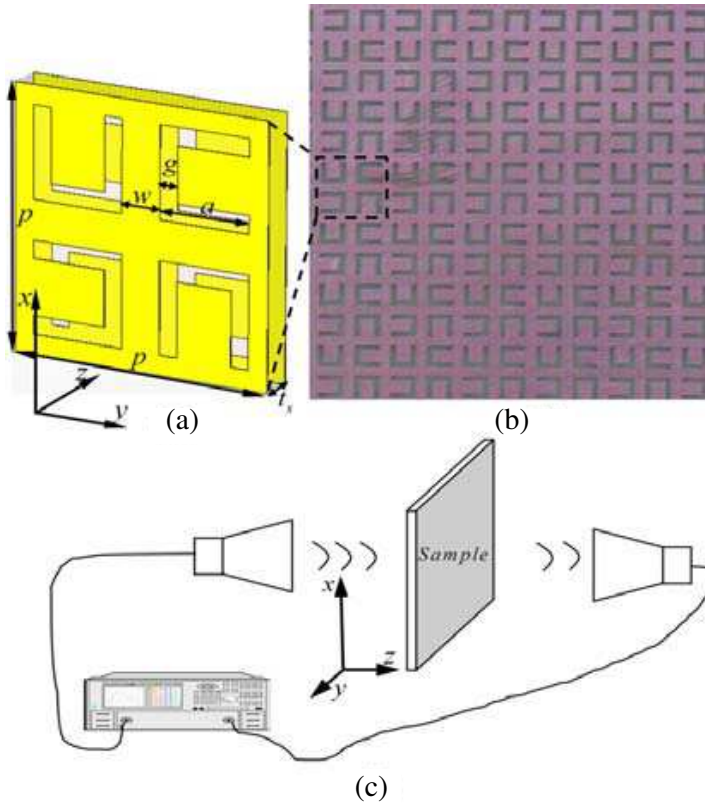


**Figure 1.** Schematics of designed CCMM structure working in microwave frequency band: (a) perspective view of the unit cell structure, (b) portion photography of the tested sample, (c) schematics of the circular polarization wave testing system.

The transmission spectra of experimental measurements were carried out in an EM anechoic chamber. Agilent PNA-X N5244A vector network analyzer connected to the two standard broadband circular horn antennae that produced LCP and RCP waves in the range of 8–18 GHz were used to measure the sample and the schematics of the circular polarization wave testing system is shown in Figure 1(c). In this testing system, the transmission magnitudes and phases of the LCP and RCP waves of the sample could be measured.

Figures 2(a) and 2(b) show the simulation (left) and experimental (right) results of transmission spectra ( $T_{--}/T_{++}$ ) for the LCP and RCP waves. The simulated transmissions of RCP and LCP waves are almost the same except for a little difference (1–2 dB) around the

two transmission dips, i.e., 12.9 GHz and 17.1 GHz, respectively. As shown in Figures 2(e) and (f), in the entire frequency of 8–18 GHz, the experimental ellipticity ( $\eta$ ) is very small and less  $1.5^\circ$ , and the  $\eta = 0$  at 15.5 GHz. Figures 2(c) and 2(d) show the simulated (left)

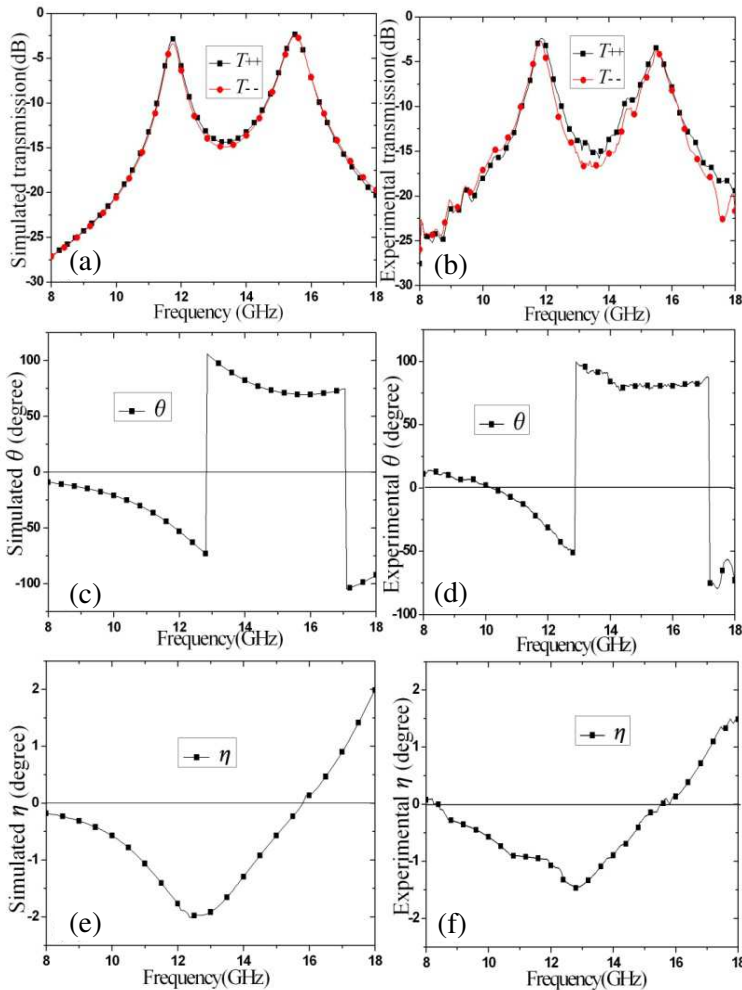


**Figure 2.** Simulated and experimental transmission results for the CCMM in microwave frequency band: (a) and (b) are the transmission spectra for RCP and LCP waves, (c) and (d) are the polarization azimuth rotation angle  $\theta$  of the transmitted wave, (e) and (f) are the ellipticity  $\eta$ , respectively.

and experimental (right) results of the polarization azimuth rotation angle ( $\theta$ ) of the transmitted wave. The calculated results nicely agree with our experimental results. At the frequency of 15.5 GHz,  $\eta = 0$  where it corresponds to a pure optical activity effect. It's mean that the CCMM can rotate a linearly polarized incident wave a certain angle  $\theta$  at this frequency. The  $\theta$  is approximately  $83^\circ$ , which exhibits stronger optical activity compared with the previously designed chiral structure [19–31], and the proposed CCMM can be used as a polarizer.

To obtain effective EM parameters of the proposed CCMM, a standard parameter retrieval method has been used [21, 38, 39], and the relative wave impedance  $z$  and refractive index  $n_+/n_-$  for RCP/LCP eigenwaves can be calculated from the simulated transmission ( $T_{++}/T_{--}$ ) and reflection ( $R = R_{++} = R_{--}$ ) [21]. Then, the other parameters can be calculated as  $n = (n_+ + n_-)/2$ ,  $\kappa = (n_+ - n_-)/2$ ,  $\mu = z(n_+ + n_-)/2$  and  $\varepsilon = (n_+ + n_-)/2z$ . As shown in Figure 3(a), it can be observed that the real part of  $n_+$  for RCP wave is negative from 12.2 GHz to 16.2 GHz, and the maximal FOM ( $-\text{Re}(n_+)/\text{Im}(n_+)$ ) is 6.2 at 12.35 GHz. For LCP wave, the real part of  $n_-$  is negative from 16.2 to 18 GHz, and the maximal FOM is about 7.1 at 16.3 GHz. Their peak values of negative refractive indices are  $-5.1$  and  $-4.2$ , respectively. If we use a loss-free dielectric, the FOM could be larger than 10 according to our numerical simulation. The negative refractive indices of the RCP/LCP eigenwaves are actually attributed by the relatively small  $n$  and large chirality  $\kappa$  [21], and the calculated the real part of  $n$  and  $\kappa$  are shown in Figure 3(b). The chirality is very large,  $\kappa = -2.15$  at  $\eta = 0$ , which corresponds to frequency of 15.5 GHz. The refractive index  $\text{Re}(n)$  is negative with dual-band from 12.3 to 13.5 GHz, and from 16.25 to 18 GHz, respectively which is similarly to its counterpart (U-shaped structure assembly) [24]. In Figures 3(c) and 3(d), we show the retrieved the effective permeability and permittivity of the CCMM. Obviously, except the tiny range around 12.2 GHz and 16.2 GHz, the  $\text{Re}(\mu)$  is always positive throughout the entire frequency range, while  $\text{Re}(\varepsilon)$  is negative above the two resonances, thus results in a dual-band negative refractive index.

To illustrate the mechanism of the chiral behaviors for the proposed CCMM, we studied the surface current distributions as shown in Figure 4. The currents are driven by the incident RCP and LCP eigenwaves at the resonance frequencies of 12.2 GHz and 16.2 GHz, respectively. From Figures 4(a) and 4(b), it can be seen that the surface currents on the upper layer and bottom layer of the CCMM structure are in the cross direction, which contribute to the weaker virtual magnetic resonance and resemble the coupling of a pair of anti-symmetrically arranged magnetic dipoles as well

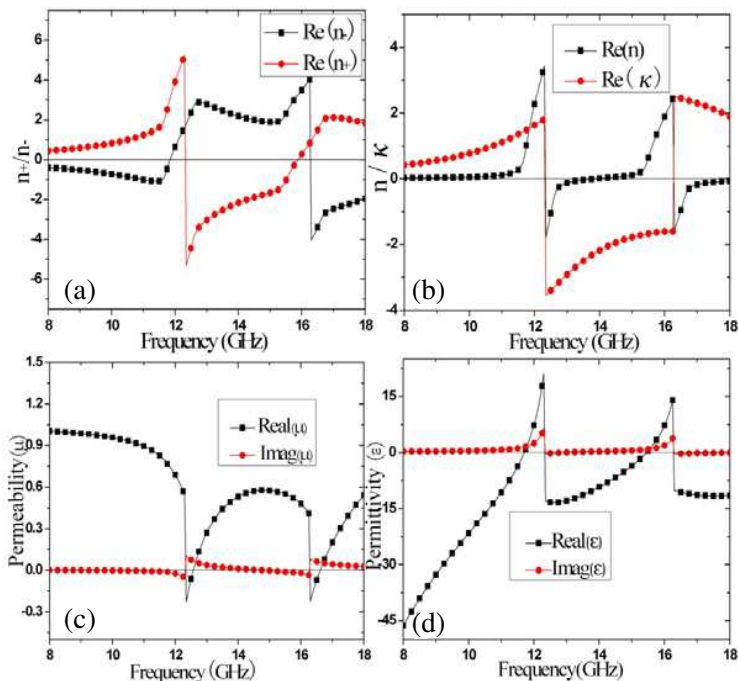


**Figure 3.** The retrieved effective parameters of the CCMM at microwave frequency: (a) the real parts of the refractive index  $n_+/n_-$  for LCP and RCP waves, (b) the real parts of the refractive index  $n$  and chiral parameter  $\kappa$ , (c) and (d) the effective permeability and permittivity.

as electric resonance [26, 27, 32]. Another way, the surface current distribution also could be explained that parallel and antiparallel surface current can be projected onto two perpendicular directions, and these pairs of surface current form magnetic and electric dipoles along specific directions [29]. The strong cross coupling between electric and magnetic field also could be attributed to chirality [33]. The currents of U-shaped slots of the metal plates are also in the opposite direction, which is due to the complementary relation with U-shaped structure CMM [24]. Comparing with the U-shaped structure assembly, this CCMM also exhibits stronger magnetoinductive and electroinductive coupling effects in resonances frequencies, finally resulting in giant optical activity and negative refractive indices [24, 36]. The coupling effects between the two complementary U-shaped structures in each pair are crucial for optical activity and negative index properties.

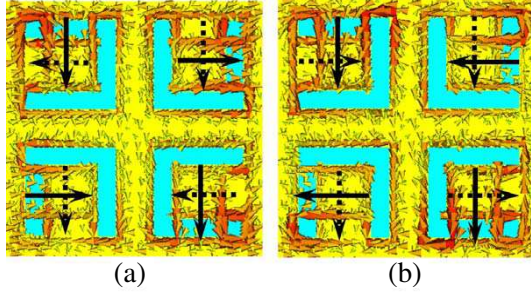


**Figure 4.** The surface current distributions of the proposed complementary structure for the RCP wave incidence at (a) 12.2 GHz and (b) LCP wave incidence at 16.2 GHz. The solid arrows denote the surface current directions for the upper layer, and the dashed arrows denote the surface current directions for the bottom layer.

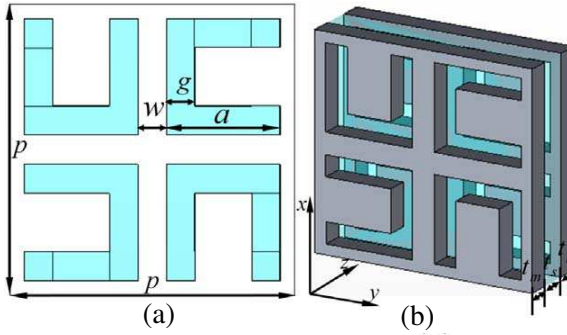


**Figure 5.** Schematics of the proposed complementary structure working at near-infrared frequency: (a) top view of the unit cell structure, (b) perspective view of the unit cell structure. The geometry parameters of the unit cell are given as  $p = 0.5 \mu\text{m}$ ,  $a = 0.2 \mu\text{m}$ ,  $g = 0.05 \mu\text{m}$ ,  $w = 0.05 \mu\text{m}$ ,  $t_s = 0.05 \mu\text{m}$ ,  $t_m = 0.065 \mu\text{m}$ .

### 3. DESIGNED STRUCTURE AND SIMULATION FOR NEAR-INFRA-RED FREQUENCY BAND

Taking a further step, we also studied the EM properties of this design at near-infrared frequency by scaling down the geometry dimension numerically. Figure 5 shows the schematic of one unit cell of the proposed complementary structure working at near-infrared frequency. Owing to the geometry dimension of the unit cell of this CCMM is much smaller than the operating wavelength ( $< \lambda/10$ ), thus without

diffraction effect in our device. In simulation model, the spacer is selected as  $\text{MgF}_2$  membrane with the relative dielectric constant of 1.9, and the gold is described by the frequency dependent Drude model with plasma frequency  $\omega_p = 1.37 \times 10^{16} \text{ s}^{-1}$  and scattering frequency  $\gamma = 2.04 \times 10^{14} \text{ s}^{-1}$  [20]. The unit cell boundary condition was applied and the circular polarized eigenwaves (LCP and RCP waves) were used directly.

Firstly, we also simulated the transmission spectra of LCP ( $T_{++}$ ) and RCP ( $T_{--}$ ) waves, as shown in Figure 6(a). We find obvious resonance dips around the frequencies of 175 THz and 230 THz. It can be observed that there are obvious differences between the transmissions of RCP and LCP waves around the resonances. Around the frequency of 175 THz, the transmission of RCP wave is about 6 dB lower than that of the LCP wave. While around the frequency of 230 THz, the transmission of RCP wave is about 9 dB higher than

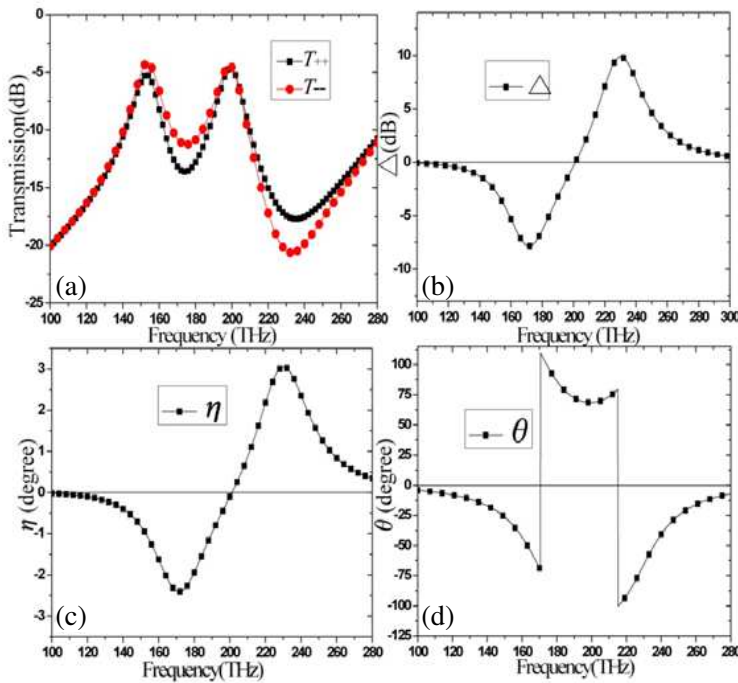


**Figure 6.** (a) Simulated results for the CCMM in the near-infrared frequency band, (a) the transmission spectra for LCP and RCP waves, (b) the circular dichroism  $\Delta$ , (c) the ellipticity angle  $\eta$ , (d) the polarization azimuth rotation angle  $\theta$ .

that of the LCP wave. Figure 6(b) shows that this complementary structure has a large circular dichroism  $\Delta$  at the two resonances, and the maximal  $\Delta$  is up to 10 dB, so the structure has distinct optical property. The retrieved ellipticity angle  $\eta$  and polarization azimuth rotation angle  $\theta$  also show that our design has notable optical performance. In Figure 6(c), the  $\eta$  very small and less  $3^\circ$  within the whole frequency range. While at the around two resonant frequencies,  $\theta$  reaches their maximum values as shown in Figure 6(d). At the frequency of 200 THz we obtain a  $\theta$  of  $71^\circ$  with  $\eta = 0$ , which is larger than the value reported in current references [19–31]. It could be found many potential applications, such as perfect linear polarizer and half-wave plate [28].

Figure 7 presents the retrieved effective parameters of the CCMM in near-infrared frequency band. As shown in Figure 7(a), for RCP wave, the real part of  $n_+$  is negative from 162 THz to 195 THz, and

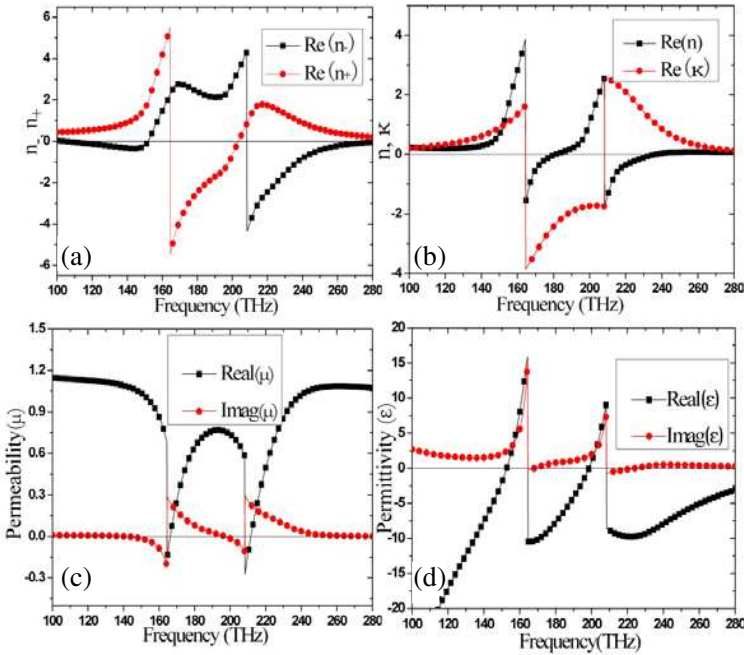


**Figure 7.** The retrieved effective parameters of the CCMM in near-infrared frequency band: (a) the real parts of the refractive index for LCP and RCP wave, (b) the real parts of the refractive index ( $n$ ) and chiral parameter  $\kappa$ , (c) and (d) the effective permittivity and permeability.

the maximal FOM is about 7.5 at 164.6 THz. While the real part of  $n_-$  is negative from 209 THz to 270 THz for LCP wave and the maximal FOM is about 7.9 at 208.4 THz. Their peak values of negative refractive indices can reach  $-5.9$  and  $-5.1$ , respectively. The main reason is that in the frequency range from 162 THz to 195 THz, the chiral parameter  $\kappa$  is negative and the absolute value is bigger than refractive index  $n$ , thus leading to  $n_+ < 0$  (see the Figure 7(b)). Similarly, in the frequency range from 209 THz to 270 THz, the  $\kappa$  is positive and the value is bigger than refractive index  $n$ , thus leading to  $n_- < 0$  (see the Figure 7(b)). We also calculated the effective permeability and permittivity as shown in Figures 7(c) and 7(d). Obviously, except the tiny range around 112 THz and 208 THz, the  $\text{Re}(\mu)$  is always positive throughout the entire frequency range, while  $\text{Re}(\varepsilon)$  is negative above the two resonances, which is consistent with the observation of  $\text{Re}(n) < 0$  from 162 to 180 THz and 208 to 245 THz as shown in Figure 7(d). These results are also similarly to the traditional design of negative refractive medium, which usually requires the real parts of the permeability ( $\mu = \mu' + i\mu''$ ) and the permittivity ( $\varepsilon = \varepsilon' + i\varepsilon''$ ) are simultaneously negative or  $\mu'\varepsilon'' + \mu''\varepsilon' < 0$  [2, 3, 40]. Thus, this structure may also have many potential applications, such as cloaking and super-lens.

#### 4. CONCLUSIONS

In summary, we have designed and studied a CCMM structure experimentally and numerically. The simulated and experimental results show that the exceptionally strong polarization rotation could be realized at 15.5 GHz. We observe experimentally a polarization rotation angle of  $83^\circ$  with  $\eta = 0$  for the proposed CCMM, which is larger than the value reported in current designed chiral structure [19–31]. Like its counterpart (U-shaped structure assembly), the dual-band negative refractive index mainly originates from the chiral configuration of this complementary structure. The mechanism of the chiral behavior at the resonance frequencies can be interpreted as stronger magnetoinductive and electroinductive coupling effects. Furthermore, this design also exhibits stronger circular dichroism, giant optical activity, and negative index in near-infrared frequency band by scaling down the geometry dimension of the unit cell. The maximal circular dichroism is up to 10 dB, and the polarization rotation angle of  $71^\circ$  with  $\eta = 0$  at 200 THz. The designed structure has excellent optical properties, and may find potential applications in the optical functional materials, cloaking, super-lens and optical polarization devices.

## REFERENCES

1. Veselago, V. G., "The electrodynamics of substances with simultaneously negative values of  $\epsilon$  and  $\mu$ ," *Sov. Phys. Usp.*, Vol. 10, No. 4, 509–514, 1968.
2. Smith D. R., W. J. Padilla, D. C. Vier, S. C. Nemat-Nasser, and S. Schultz, "Composite medium with simultaneously negative permeability and permittivity," *Phys. Rev. Lett.*, Vol. 84, No. 18, 4184–4187, 2000.
3. Shelby R. A., D. R. Smith, and S. Schultz, "Experimental verification of a negative index of refraction," *Science*, Vol. 292, 77–79, 2001.
4. Pendry, J. B., "Negative refraction makes a perfect lens," *Phys. Rev. Lett.*, Vol. 85, No. 18, 3966–3969, 2000.
5. Schurig, D., J. J. Mock, B. J. Justice, S. A. Cummer, J. B. Pendry, A. F. Starr, and D. R. Smith, "Metamaterial electromagnetic cloak at microwave frequencies," *Science*, Vol. 314, No. 5801, 977–980, 2006.
6. Ziolkowski, R. W. and A. Erentok, "Metamaterial-based efficient electrically small antennas," *IEEE Trans. on Antenn. and Propag.*, Vol. 54, No. 7, 2113–2130, 2006.
7. Mirza, I. O., S. Shi, and D. W. Prather, "Phase modulation using dual split ring resonators," *Opt. Express*, Vol. 17, No. 7, 5089–5097, 2009.
8. Zhang, S., W. Fan, K. J. Malloy, S. R. Brueck, N. C. Panoiu, and R. M. Osgood, "Near-infrared double negative metamaterials," *Opt. Express*, Vol. 13, No. 13, 4922–4930, 2005.
9. Shalaev, V. M., W. Cai, U. K. Chettiar, H. K. Yuan, A. K. Sarychev, V. P. Drachev, and A. V. Kildishev, "Negative index of refraction in optical metamaterials," *Opt. Lett.*, Vol. 30, No. 24, 3356–3358, 2005.
10. Paul, O., C. Imhof, B. Reinhard, R. Zengerle, and R. Beigang, "Negative index bulk metamaterial at terahertz frequencies," *Opt. Express*, Vol. 16, No. 9, 6736–6744, 2008.
11. Tretyakov, S., I. Nefedov, A. Sihvola, S. Maslovski, and C. Simovski, "Waves and energy in chiral nihility," *Journal of Electromagnetic Waves and Applications*, Vol. 17, No. 5, 695–706, 2003.
12. Pendry, J. B., "A chiral route to negative refraction," *Science*, Vol. 306, No. 5700, 1353–1355, 2004.
13. Rogacheva, A. V., V. A. Fedotov, A. S. Schwanecke, and

- N. I. Zheludev, "Giant gyrotropy due to electromagnetic-field coupling in a bilayered chiral structure," *Phys. Rev. Lett.*, Vol. 97, No. 17, 177401, 2006.
14. Liu, H., D. A. Genov, D. M. Wu, Y. M. Liu, Z. W. Liu, C. Sun, S. N. Zhu, and X. Zhang, "Magnetic plasmon hybridization and optical activity at optical frequencies in metallic nanostructures," *Phys. Rev. B*, Vol. 76, No. 7, 073101(4), 2007.
  15. Li, T. Q., H. Liu, T. Li, S. M. Wang, F. M. Wang, R. X. Wu, P. Chen, S. N. Zhu, and X. Zhang, "Magnetic resonance hybridization and optical activity of microwaves in a chiral metamaterial," *Appl. Phys. Lett.*, Vol. 92, No. 13, 131111(3), 2008.
  16. Decker, M., S. Linden, and M. Wegener, "Coupling effects in low-symmetry planar split-ring resonator arrays," *Opt. Lett.*, Vol. 34, No. 10, 1579–1581, 2009.
  17. Wang, B., T. Koschny, and C. M. Soukoulis, "Wide-angle and polarization-independent chiral metamaterial absorber," *Phys. Rev. B*, Vol. 80, No. 3, 033108, 2009.
  18. Singh, R. J., E. Plum, W. L. Zhang, and N. I. Zheludev, "Highly tunable optical activity in planar achiral terahertz metamaterials," *Opt. Express*, Vol. 18, No. 13, 13425–13430, 2010.
  19. Wang, B., T. Koschny, M. Kafesaki, and C. M. Soukoulis, "Chiral metamaterials: Simulations and experiments," *J. Opt. A: Pure Appl. Opt.*, Vol. 11, 114003(10), 2009.
  20. Zhang, S., Y.-S. Park, J. Li, X. Lu, W. Zhang, and X. Zhang, "Negative refractive index in chiral metamaterials," *Phys. Rev. Lett.*, Vol. 102, No. 2, 023901(4), 2009.
  21. Plum, E., J. Zhou, J. Dong, V. A. Fedotov, T. Koschny, C. M. Soukoulis, and N. I. Zheludev, "Metamaterial with negative index due to chirality," *Phys. Rev. B*, Vol. 79, No. 3, 035407(6), 2009.
  22. Zhou, J., J. Dong, B. Wang, T. Koschny, M. Kafesaki, and C. M. Soukoulis, "Negative refractive index due to chirality," *Phys. Rev. B*, Vol. 79, No. 12, 121104(4), 2009.
  23. Dong, J., J. Zhou, T. Koschny, and C. Soukoulis, "Bi-layer crosschiral structure with strong optical activity and negative refractiveindex," *Opt. Express*, Vol. 17, No. 16, 14172–14179, 2009.
  24. Li, Z., R. Zhao, T. Koschny, M. Kafesaki, K. B. Alici, E. Colak, H. Caglayan, E. Ozbay, and C. M. Soukoulis, "Chiral metamaterials with negative refractive index based on four "U" split ring resonators," *Appl. Phys. Lett.*, Vol. 97, No. 8, 081901(3), 2010.

25. Decker, M., R. Z., C. M. Soukoulis, S. Linden, and M. Wegener, "Twisted split-ring-resonator photonic metamaterial with huge optical activity," *Opt. Lett.*, Vol. 35, No. 10, 1593–1593, 2010.
26. Zhao, R., L. Zhang, J. Zhou, T. Koschny, and C. M. Soukoulis, "Conjugated gammadion chiral metamaterial with uniaxial optical activity and negative refractive index," *Phys. Rev. B*, Vol. 83, No. 3, 035105(4), 2011.
27. Li, Z., K. B. Alici, E. Colak, and E. Ozbay, "Complementary chiral metamaterials with giant optical activity and negative refractive index," *Appl. Phys. Lett.*, Vol. 98, 161907, 2011.
28. Li, J., F. Q. Yang, and J. F. Dong, "Design and simulation of L-shaped chiral negative refractive index structure," *Progress In Electromagnetics Research*, Vol. 116, 395–408, 2011.
29. Wu, Z., J. Zhu, H. Lu, and B. Zeng, "A double-layer metamaterial with negative refractive index originating from chiral configuration," *Microw. Opt. Technol. Lett.*, Vol. 53, No. 1, 163–166, 2011.
30. Zarifi, D., M. Soleimani, and V. Nayyeri, "A novel dual-band chiral metamaterial structure with giant optical activity and negative refractive index," *Journal of Electromagnetic Waves and Applications*, Vol. 26, Nos. 2–3, 251–263, 2012.
31. Li, Z., K. B. Alici, H. Caglayan, M. Kafesaki, C. M. Soukoulis, and E. Ozbay, "Composite chiral metamaterials with negative refractive index and high values of the figure of merit," *Opt. Express*, Vol. 20, No. 16, 6146–6156, 2012.
32. Zhao, R., T. Koschny, E. N. Economou, and C. M. Soukoulis, "Comparison of chiral metamaterial designs for repulsive Casimir force," *Phys. Rev. B*, Vol. 81, No. 32, 235126, 2010.
33. Jackson, J. D., *Classical Electrodynamics*, 3rd Edition, Wiley, 1999.
34. Falcone, F., T. Lopetegui, M. A. G. Laso, J. D. Baena, J. Bonache, M. Beruete, R. R. Marques, F. F. Martinez, and M. Sorolla, "Babinet principle applied to the design of metasurfaces and metamaterials," *Phys. Rev. Lett.*, Vol. 3, No. 19, 197401(4), 2004.
35. Zentgraf T., T. P. Meyrath, A. Seidel, S. Kaiser, and H. Giessen, "Babinet's principle for optical frequency metamaterials and nanoantennas," *Phys. Rev. B*, Vol. 76, No. 3, 033407(4), 2007.
36. Liu, N., S. Kaiser, and H. Giessen, "Magnetoinductive and electroinductive coupling in plasmonic metamaterial molecules," *Adv. Mater.*, Vol. 20, No. 23, 4521–4525, Deerfield Beach, Florida, 2008.

37. Xiong, X., W. H. Sun, Y. J. Bao, M. Wang, R. W. Peng, C. Sun, X. Lu, J. Shao, Z. F. Li, and N. B. Ming, "Construction of a chiral metamaterial with a U-shaped resonator assembly," *Phys. Rev. B*, Vol. 81, No. 7, 075119, 2010.
38. Zhao, R., T. Koschny, and C. M. Soukoulis, "Chiral metamaterials: Retrieval of the effective parameters with and without substrate," *Opt. Express*, Vol. 8, No. 14, 14553–14567, 2010.
39. Kwon, D., D. H. Werner, A. V. Kildishev, and V. M. Shalaev, "Material parameter retrieval procedure for general bi-isotropic metamaterials and its application to optical chiral negative-index metamaterial design," *Opt. Express*, Vol. 16, No. 16, 11822–11829, 2008.
40. Depine, R. A. and A. A. Lakhtakia, "New condition to identify isotropic dielectric-magnetic materials displaying negative phase velocity," *Microw. Opt. Technol. Lett.*, Vol. 41, No. 4, 315–316, 2004.